Vol 13 No 7, July 2004
1009-1963/2004/13(07)/1144-05

Chinese Physics

© 2004 Chin. Phys. Soc.
and IOP Publishing Ltd

Magnetic properties and coercivity mechanism of precipitation-hardened Gd–Co based ribbons*

Rong Chuan-Bing(荣传兵)†, Zhang Jian(张 健), Du Xiao-Bo(杜晓波),
Zhang Hong-Wei(张宏伟), Zhang Shao-Ying(张绍英), and Shen Bao-Gen(沈保根)

State Key Laboratory of Magnetism, Institute of Physics and Centre for Condensed Matter Physics, Chinese Academy of Sciences, Beijing 100080, *China*

(Received 27 November 2003; revised manuscript received 25 December 2003)

$Gd(Co_{0.88-x}Cu_xFe_{0.09}Zr_{0.03})_z$ ribbons with $x = 0.075 - 0.200$ and z=6.4–7.7 have been prepared by a melt-spinning technique. A cellular microstructure consisting of 2:17 cells surrounded by the 1:5 cell boundary phase is obtained after precipitation hardening. The dependence of room temperature coercivity on the heat treatment process suggests that the long-time isothermal aging is not helpful for the development of magnetic properties. Positive temperature coefficient of remanence from room temperature to about 673K is typical for all samples, while positive temperature coefficient of coercivity is obtained only in ribbons with low Cu content. The coercivity mechanism of the precipitation-hardened ribbons at different temperatures is also discussed.

Keywords: precipitation hardening, high-temperature magnetic properties, coercivity mechanism
PACC: 7550V, 7560E, 7550B, 8140C

1. Introduction

Precipitation-hardened $Sm(Co,Fe,Cu,Zr)_z$ magnets are characterized by large anisotropy fields and high Curie temperatures, which make them suitable candidates for high-temperature applications.[1] However, both coercivity H_c and remanence J_r decrease with increasing temperature in traditional permanent magnets.[2,3] To improve the high-temperature magnetic properties, numerous works have been performed on the temperature coefficients of remanence $\alpha(= dJ_r/dT)$. The investigations[4,5] show that it is possible to control α in a certain temperature range when Sm is partially substituted with heavy rare earth (HRE). The Gd-substituted magnets can provide maximum energy product $(BH)_{max}$ of about 127–135kJ/m^3 in the temperature range of 293–473K.[6] Another feature particularly important with respect to application is the low-temperature coefficient of coercivity β $(=d(\mu_0 H_c)/dT)$ at elevated temperatures. Recently, small negative or even positive β has been achieved in several works by adjusting the composition of magnets and heat treatment condition.[7–10] The abnormal temperature dependence of coercivity results from the coexistence of a cellular microstructure with rhombohedral 2:17-type cells surrounded by a Cu-rich 1:5-type cell boundary phase.[7–12] Besides Sm–Co, Y–Co[11] and Pr–Co[12] systems also have positive β when the planar anisotropy of 2:17 phase was transformed into the uniaxial. In this work, we report a Gd–Co based ribbon which possesses positive α and β simultaneously.

2. Experiment

Ingots with nominal composition $Gd(Co_{0.88-x}Cu_x Fe_{0.09}Zr_{0.03})_z$ ($x = 0.075-0.200$, z=6.4–7.7) were prepared by arc-melting. Pieces of ingots were then inserted into a quartz tube with a nozzle. The chamber was evacuated to a vacuum of 10^{-2} Pa and then filled with high-purity argon. The samples were induction melted and ejected through the nozzle using a pressure difference. The surface speed of the Cu wheel was 15m/s. The ribbons were subsequently isothermally aged at 1123K for 0–20h followed by slow cooling at 1K/min to 673K. Crystalline structure was determined by x-ray diffraction (XRD) with Cu Kα radiation. Microstructure was analysed by transmission electron microscopy (TEM). The magnetic properties

*Project supported by the National High Technology Development Programme of China (Grant No 2001AA324019).
†E-mail: rongcb@g203.iphy.ac.cn

at room temperature (RT) were obtained using a superconducting quantum interference device (SQUID) magnetometer with a maximum applied field of 5T. High-temperature magnetic properties were measured using a vibrating sample magnetometer (VSM). The field was applied along the longitudinal direction of the ribbon so that demagnetization factor could be neglected.

3. Results and discussion

3.1. Microstructure analysis

Figure 1 gives the XRD patterns of the melt-spun and precipitation-hardened $Gd(Co_{0.73}Cu_{0.15}Fe_{0.09}Zr_{0.03})_z$ ribbons. As can be seen, the as-spun ribbon exhibits a nearly single 1:7 phase structure and is composed of a two-phase mixture of 1:5 and 2:17 after precipitation hardening. The characteristic peaks of the 1:5 and 2:17 structure are marked by an asterisk and a plus sign, respectively. The broadened peaks of the precipitation-hardened samples indicate that the phase transformation leads to the formation of a fine microstructure. The intensity of 1:5 peaks grows while that of 2:17 peaks decreases with decreasing of z. This means that the volume fraction of 1:5 phase increases with decrease of z. TEM analysis shows that a cellular microstructure, which is similar to that of sintered magnet,[7,8] is obtained after precipitation hardening. A more detailed report on the microstructure will be published elsewhere.

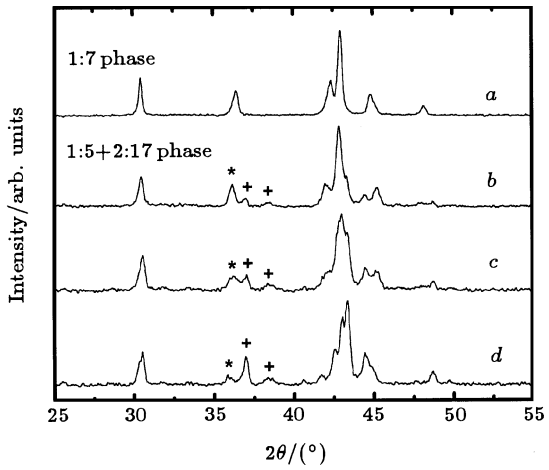


Fig.1. XRD patterns of $Gd(Co_{0.73}Cu_{0.15}Fe_{0.09}Zr_{0.03})_z$ (z=6.4–7.7) ribbons. curve *a* as-spun, z=7.0; *b* precipitation-hardened, z=6.4; *c* precipitation-hardened, z=7.0; *d* precipitation-hardened, z=7.7.

3.2. Magnetic properties

Cu content has an important effect on the magnetic properties of the precipitation-hardened magnets.[7] Figure 2 shows the dependence of RT coercivity of $Gd(Co_{0.88-x}Cu_xFe_{0.09}Zr_{0.03})_z$ ribbons on the Cu content. It is noted that more Cu is required to reach the maximum RT coercivity with decreasing of z. The energy-dispersive x-ray spectroscopy reveals that the 1:5 cell boundary phase contains more Cu than the 2:17 cells. Since a lower z-value means a larger amount of the 1:5 phase as discussed above, more Cu is required for the same optimum Cu content in the 1:5 phase. This behaviour is in agreement with the results in the Sm–Co and Y–Co based magnets.[7,11]

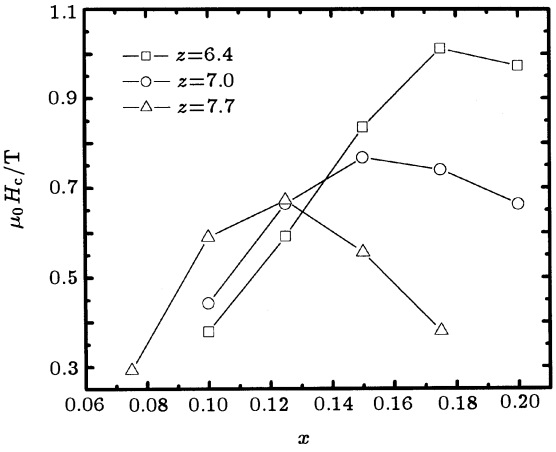


Fig.2. RT coercivity of $Gd(Co_{0.88-x}Cu_xFe_{0.09}Zr_{0.03})_z$ ribbons as a function of Cu content x for different values of z. The ribbons have been aged at 1123K for 10h.

The effect of the isothermal aging time t_a on the RT coercivity of $Gd(Co_{0.88-x}Cu_xFe_{0.09}Zr_{0.03})_{7.0}$ ribbons is presented in Fig.3. It is found that H_c is not very sensitive to t_a for the samples with low Cu content. However, H_c decreases dramatically with increasing t_a for the high Cu content samples. The decrease of H_c may be due to the appearance of the large cell which is observed in the TEM micrographs. It suggests that the long-time isothermal aging is not helpful for the development of magnetic properties. This result is important technologically for the fabrication of more economical precipitation-hardened magnets.

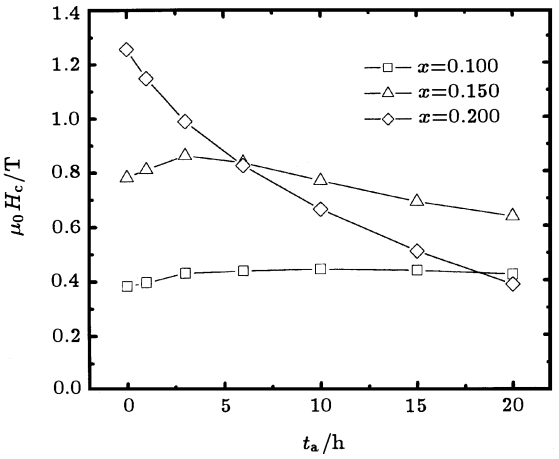


Fig.3. RT coercivity as a function of aging time t_a for $Gd(Co_{0.88-x}Cu_xFe_{0.09}Zr_{0.03})_{7.0}$ ribbons with different Cu content x.

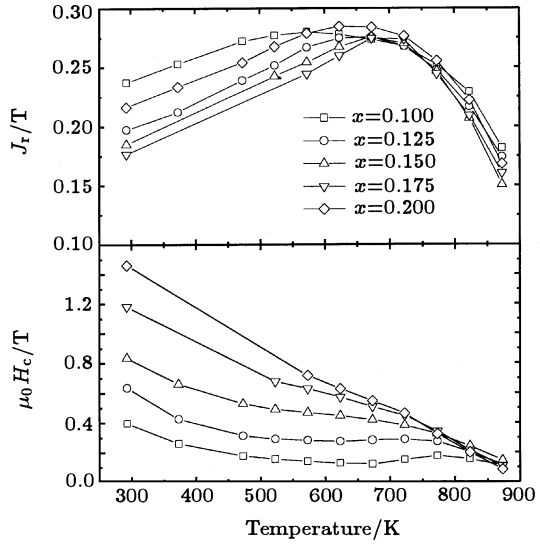


Fig.4. Temperature dependences of remanence and coercivity of $Gd(Co_{0.88-x}Cu_xFe_{0.09}Zr_{0.03})_{6.4}$ (x = 0.100 – 0.200) samples without isothermal aging.

Figure 4 shows the temperature dependences of remanence and coercivity of $Gd(Co_{0.88-x}Cu_xFe_{0.09}Zr_{0.03})_{6.4}$ ribbons obtained by simply slow cooling the as-spun ribbons from 1123K to 673K. All samples exhibit a positive α from RT to about 673K. The magnetic moment coupling of the Gd sublattice is anti-parallel to the Co sublattice whereas for the light rare earths they are parallel. Although in both cases the rare earth sublattice disorders rapidly with increase of temperature, the ferrimagnetic coupling of Gd–Co magnets results in an increasing magnetization with increasing temperature over the temperature range of interest.[1,4,5] However, positive or zero β is observed only in ribbons with $x \leq 0.125$. Further addition of Cu causes the monotonic dependence of H_c on temperature. The temperature dependences of J_r and H_c for the samples with z=7.0 and 7.7 resemble those of ribbons with z=6.4 shown in Fig.4. The positive α and β are helpful to design the high-temperature magnets.

3.3. Coercivity mechanism

Stoner–Wohlfarth theory shows that there is a simple relationship between $J_d(H)$ and $J_r(H)$:[13]

$$J_d(H) = J_r(\infty) - 2J_r(H), \quad (1)$$

where the remanent $J_r(H)$ is acquired after the application and subsequent removal of a direct field H; $J_d(H)$ after DC saturation in one direction and subsequent application and removal of a direct field H in the reverse direction. $J_r(\infty)$ is denoted as J_r for convenience. The above relationship should hold true for non-interacting single domain particles or uniform domain wall pinning where the domain walls encounter the same type of pins in the initial magnetization and demagnetization state.

In nanocrystalline magnets, the intergrain exchange coupling plays an important role during the magnetization reversal process and always leads to the remanence enhancement.[14–16] The relation

$$\delta m(H) = [J_d(H) - J_r(\infty) + 2J_r(H)]/J_r(\infty) \quad (2)$$

can be adopted to determine the strength of exchange-coupling interactions in a real system.[17–19] Positive values of $\delta m(H)$ are due to interactions promoting the magnetized state, while negative values of $\delta m(H)$ are caused by interaction tending to assist magnetization reversal. The curve of $\delta m(H)$ versus H is often called the Henkel plot.[17] Figure 5 shows $\delta m(H)$ plots of the $Gd(Co_{0.73}Cu_{0.15}Fe_{0.09}Zr_{0.03})_{7.0}$ ribbons aged at 1123K for 0 and 20h, respectively. The intergrain exchange coupling decreases slightly with increasing isothermal aging time. This may be attributed to the appearance of large cells in the ribbon after long-time aging. The coercivity mechanism of uniform domain wall pinning can be excluded due to the existence of nonzero $\delta m(H)$.

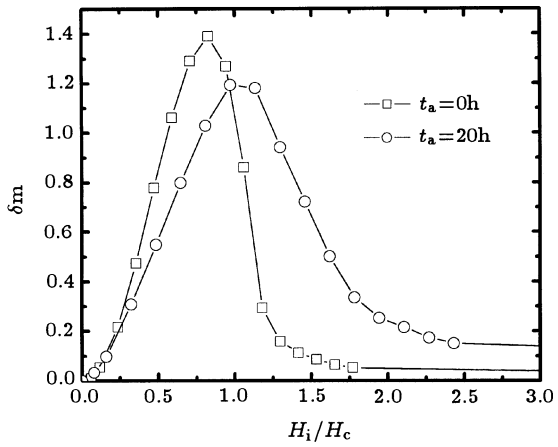


Fig.5. Henkel plots of $Gd(Co_{0.73}Cu_{0.15}Fe_{0.09}Zr_{0.03})_{7.0}$ ribbons aged at 1123K for 0 and 20h, respectively.

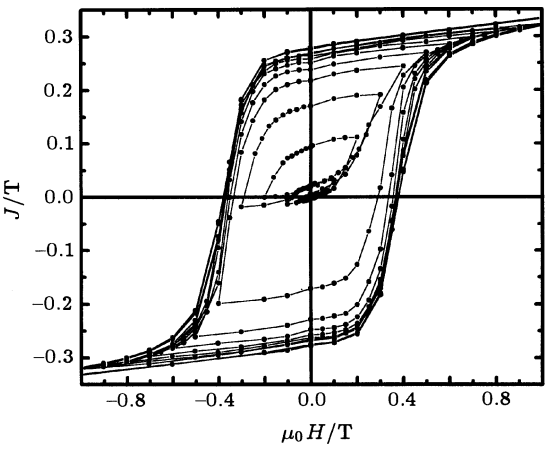


Fig.6. Minor hysteresis loops at RT of the $Gd(Co_{0.73}Cu_{0.15}Fe_{0.09}Zr_{0.03})_{7.0}$ ribbon with increasing field and major hysteresis loop at 5T.

Traditionally, the field dependence of H_c on maximum applied field H^{max} is different for nucleation and domain wall pinning. H_c increases linearly with magnetizing and then saturates for the nucleation model, while it is almost negligible up to a critical field above which it suddenly increases to saturation.[20] Figure 6 shows the typical minor hysteresis loops at RT of the $Gd(Co_{0.73}Cu_{0.10}Fe_{0.09}Zr_{0.03})_{7.0}$ ribbon with increase of H^{max}. The minor loops show very small coercivity and remanence as $\mu_0 H^{max} \leq 0.1$T. With further increasing H^{max}, coercivity and remanence elevate obviously. This is the special characteristic of the domain wall pinning mechanism. The significantly asymmetric minor loops ($0.1T \leq H^{max} \leq 0.3T$) mean that strong inhomogeneous pinning centres exist in the samples. Plots of H_c versus H^{max} at different temperatures of the $Gd(Co_{0.88-x}Cu_xFe_{0.09}Zr_{0.03})_{7.0}$ samples (x=0.10 and 0.20) are shown in Fig.7. For samples with low Cu content, the magnetization reversal is controlled by domain wall pinning at temperatures ranging from RT to 873K. The large difference between positive and negative magnetization directions at RT is caused by strong inhomogeneous pinning. The coercivity of the samples with high Cu content seems to be mainly controlled by domain wall inhomogeneous pinning, while nucleation cannot be neglected at the same time.

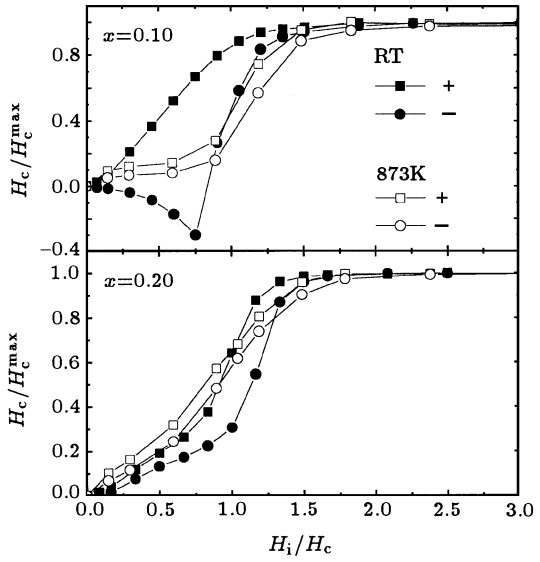


Fig.7. Coercivity vs maximum applied field for $Gd(Co_{0.88-x}Cu_xFe_{0.09}Zr_{0.03})_{7.0}$ samples (x = 0.10 and 0.20) at different temperatures. The coercivity obtained from the minor loop. Symbol '+' represents the values obtained in the second quadrant and '−' those in the fourth quadrant.

Thus, the temperature dependence of the coercivity can be explained as follows. According to the pinning mechanism,[21] the coercivity is proportional to the difference between the domain wall energies $\gamma = \sqrt{AK_1}$ for the two phases, where K_1 is the anisotropy constant and A is the exchange constant. Earlier studies showed that K_1 of 1:5 alloys decreases with increasing Cu content.[22] Thus, Cu enrichment in the 1:5 boundary phase leads to a low domain wall energy. For the ribbons with low Cu content, the coercivity is caused by a repulsive interaction between domain walls and the cell boundaries at RT ($\gamma_{2:17} < \gamma_{1:5}$). The interaction becomes attractive above some temperature T_0, where $\gamma_{2:17} > \gamma_{1:5}$. This causes an increase in H_c from T_0 to the Curie temperature of the 1:5 phase ($T_c^{1:5}$). Thus, the abnormal temperature dependence of coercivity of the samples with low Cu content can be approximately predicted by the domain wall pinning mechanism. The samples with high Cu content have $\gamma_{2:17} > \gamma_{1:5}$ in the whole

temperature range. The coercivity is always caused by an attractive domain wall pinning and has a monotonic temperature dependence.

4. Conclusion

The effects of Cu content and aging time on the magnetic properties of precipitation-hardened $Gd(Co_{0.88-x}Cu_xFe_{0.09}Zr_{0.03})_z$ ribbons ($x = 0.075 - 0.20$ and z=6.4–7.7) have been studied systematically. The structure of the as-spun ribbon is 1:7. A cellular microstructure consisting of 2:17 cells and 1:5 cell boundary phase is obtained after precipitation hardening. More Cu is needed for the same optimum Cu content in the 1:5 phase with decreasing z (i.e. increasing volume fraction of the 1:5 phase). The long-time isothermal aging is not helpful for the development of high-performance magnets. Positive α is typical for all ribbons from room temperature to about 673K, while positive β is observed only in samples with low Cu content. Plots of coercivity versus maximum applied field show that the abnormal temperature dependence of coercivity can be approximately predicted by the domain wall pinning mechanism.

References

[1] Wohlfarth E P and Buschow H J 1988 *Ferromagnetic Materials* vol 4 (Amsterdam: North-Holland) p131

[2] Zhang H W, Zhang S Y, Shen B G, Goll D and Kronmuller H 2001 *Chin. Phys.* **10** 1169

[3] Zhang H W, Rong C B, Zhang J, Zhang S Y and Shen B G 2003 *Acta Phys. Sin.* **52** 722 (in Chinese)

[4] Walmer M S, Chen C H, Walmer M H, Liu S and Kuhl G E 1998 *Proc. 15th Int. Workshop on REPM* p689

[5] Li D, Liu J, Zhou S, Jin X and Xu E 1983 *Proc. 7th Int. Workshop on Rare Earth Permanent Magnets and Their Applications* (Beijing: China Academic) p495

[6] Liu S, Ray A E and Mildrum H F 1990 *J. Appl. Phys.* **67** 4975

[7] Hadjipanayis G C, Tang W, Zhang Y, Chui S T, Liu J F, Chen C and Kronmuller H 2000 *IEEE. Trans. Magn.* **36** 3382

[8] Liu J F, Chui T, Dimitrov D and Hadjipanayis G C 1998 *Appl. Phys. Lett.* **73** 3007

[9] Goll D, Kleinschroth I, Sigle W and Kronmuller H 2000 *Appl. Phys. Lett.* 76 1054

[10] Zhou J, Skomski R, Chen C, Hadjipanayis G C and Sellmyer D J 2000 *Appl. Phys. Lett.* **77** 1514

[11] Gabay A M, Tang W, Zhang Y and Hadjipanayis G C 2001 *Appl. Phys. Lett.* **78** 1595

[12] Zhang J, Liu H, Rong C B, Zhang H W, Zhang S Y, Shen B G, Bai Y Q and Li B H 2003 *Appl. Phys. Lett.* **83** 1172

[13] Wohlfarth E P 1958 *J. Appl. Phys.* **29** 595

[14] Zhang H W, Rong C B, Zhang J, Zhang S Y and Shen B G 2002 *Phys. Rev.* B **66** 184436

[15] Fishcher R, Schrefl T, Kronmuller H and Fidler J 1996 *J. Magn. Magn. Mater* **153** 35

[16] Zhang H W, Rong C B, Zhang J, Zhang S Y and Shen B G 2003 *Acta Phys. Sin.* **52** 718 (in Chinese)

[17] Kelly P E, Grady K O, Mayo P I and Chantrell R W 1989 *IEEE. Trans. Magn.* **25** 3881

[18] Zhang H W, Zhao T Y, Rong C B, Zhang S Y, Han B S and Shen B G 2003 *J. Magn. Magn. Mater* **267** 224

[19] Du X B, Zhang H W, Rong C B, Zhang J, Zhang S Y, Shen B G, Yan Y and Jin H M 2004 *Chin. Phys.* **13** 552

[20] Hadjipanayis G C and Kim A 1988 *J. Appl. Phys.* **63** 3310

[21] Livingston J D and Martin D L 1977 *J. Appl. Phys.* **48** 1350

[22] Lectard E, Allibert C H and Ballou R 1994 *J. Appl. Phys.* **75** 6277